Cp*RuCl-Vinyl Carbenes: Two Faces and the Bifunctional Role in Catalytic Processes

Damián Padín, Jesús A. Varela* and Carlos Saá*[a]

Abstract: Ruthenium vinyl carbenes derived from Cp/Cp*RuCl-based complexes have been routinely invoked as key intermediates in tandem reactions involving a carbene/alkyne metathesis (CAM). A priori, these intermediates resemble the Grubbs-type family of catalysts, but they exhibit a completely different reactivity pattern that few, if any, other catalytic system can reproduce so far. The reactivity of these species with α-unsubstituted and α-substituted alkynals showcases the peculiarities of these intermediates. While *Z*-vinyl dihydrooxazines are preferentially obtained with the former, *Z*-vinyl epoxypyrrolidines are obtained with the latter. A combination of spectroscopic and computational data now prove that a η^3-coordination mode of the ruthenium vinyl carbene and the presence of a Lewis basic chloride ligand give rise to two markedly different stereoelectronic faces that are responsible for the unconventional reactivity of these species.

Introduction

Organometallic catalysis involving metal carbenes could be considered as a milestone in organic synthesis. Chemical reactions such as olefin metathesis,[1] cyclopropanation,[2] ylide formation,[3] cross-coupling[4] or C-H bond functionalization[5] are, nowadays, fundamental transformations in the organic chemistry laboratory. From a synthetic point of view, tandem (or cascade) processes of catalytic metal carbenes are particularly relevant due to the rapid generation of molecular complexity in a single step.[6] In this context, carbene/alkyne metathesis (CAM) leading to reactive metal vinyl carbene intermediates has emerged as a powerful tool for the construction of highly functionalized polycyclic structures.[7] On the one hand, dirhodium(II)-based catalytic systems have clearly dominated the field due to the mild reaction conditions required for carbene formation and the possibility to easily tune the reactivity and stereoselectivity by ligand modification (Figure 1a).[8] However, the high electrophilicity of rhodium carbenes and the limited coordination capabilities of dirhodium paddlewheel complexes may render the CAM step slower than other side reactions (carbene dimerization, Bamford-Stevens reaction, unselective nucleophilic attacks, etc.), thus, restricting the development of new methodologies to intramolecular reactions.[9] On the other hand, Grubbs-type ruthenium carbenes are known to be suitable complexes for inter- and intramolecular CAM processes (enyne metathesis),[10] but the low electrophilicity that makes them highly chemoselective for metathesis, avoids their use in other tandem CAM (Figure 1b). Alternatively, our research group and others have been reporting the use of Cp/Cp*RuCl-based complexes for the catalytic generation of ruthenium vinyl carbenes from alkynes and diazocompounds via intermolecular CAM (Figure 1c).[11] These intermediates can lead to dienes,[12] cyclopropanes,[13] C-H insertion products[14] or ylide intermediates which eventually afford benzoxazines,[15] furans,[16] vinyl dihydropyrans/dihydrooxazines[17] and vinyl epoxypyrrolidines.[18] Remarkably, Cp*/CpRuCl-based complexes were the only complexes to give productive tandem CAM processes.

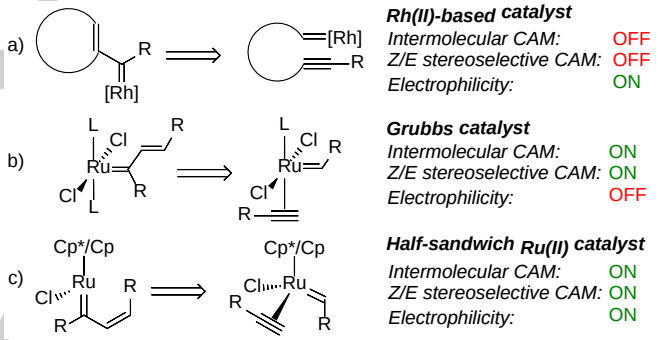

Figure 1. Reactivity and properties of rhodium and ruthenium carbenes and their CAM-derived vinyl carbenes.

Interestingly, during our studies of the reactivity of aza-alkynals with diazocompounds in the presence of Cp/Cp*RuCl-based complexes,[17-18] we observed that the formation of vinyl dihydrooxazines and vinyl epoxypyrrolidines is only determined by a subtle modification of the starting aza-alkynal (Scheme 1). Apparently, the presence or absence of substitution at α position dictates, in a highly chemoselective manner, which reaction pathway the proposed ruthenium vinyl carbene intermediate must follow. In virtue of these findings we hypothesized that geometrical and/or electronic effects after vinyl carbene formation are responsible of the different reactivity towards aldehydes.

[a] Dr. D. Padín, Prof. J. A. Varela, Prof. C. Saá
Centro Singular de Investigación en Química Biolóxica e Materiais Moleculares (CiQUS)
Departamento de Química Orgánica
Universidade de Santiago de Compostela
15782 Santiago de Compostela (Spain)
E-mail: carlos.saa@usc.es

Supporting information for this article is given via a link at the end of the document.

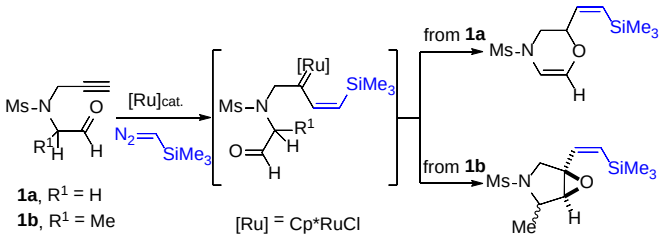

Scheme 1. Divergent behavior of catalytic ruthenium vinyl carbenes towards aldehydes.

In our aim to gain further insights into the divergent behavior of catalytic ruthenium vinyl carbenes towards aldehydes, herein, we present a deep theoretical and experimental study for the dichotomous formation of dihydrooxazines and epoxypyrrolidines as well as the first experimental evidence for the formation of reactive ruthenium η^3-vinylcarbenes from alkynes and diazo compounds.

Results and Discussion

A series of experimental studies and DFT calculations at the ωb97XD/ccPVTZpp (Ru), 6-311++G(d,p) (all other atoms)-SMD (diethylether)//ωb97XD/Lanl2dz (Ru), 6-31G(d,p) (all other atoms)-SMD (diethylether) level of theory[19] using the Gaussian 09 package[20] were performed to understand the basic principles that govern the reactivity of ruthenium vinyl carbenes derived from CAM processes catalyzed by Cp/Cp*RuCl-based complexes.

Experimental evidence for the formation of reactive Ru η^3-vinylcarbenes

The description of ruthenium η^1-vinylcarbenes of type **4** (Figure 2) has been traditionally ligated to the development of well-defined precatalysts for olefin metathesis.[21] The group of Grubbs clearly demonstrated that η^1 coordination is crucial for catalytic activity since η^3-vinylcarbenes of type **5** were poorly reactive in the polymerization of diphenylacetylene and completely unreactive in ring closing metathesis.[22] These results were later confirmed computationally by Straub and coworkers.[23] Interestingly, the half-sandwich binuclear ruthenium η^1-vinylcarbene **6** was also a catalytically competent complex for ROMP of strained olefins, but much less active than typical Grubbs-type catalysts.[21b] Although most efforts were originally focused in the development of better ruthenium precatalysts for olefin metathesis, little attention was paid to understand the requirements needed to develop other tandem reactions involving CAM processes.

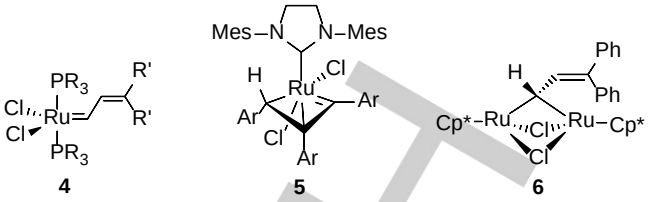

Figure 2. Precedents in the isolation and characterization of ruthenium vinyl carbenes.

The successful results obtained by Fürstner and coworkers in the isolation and characterization of ruthenium carbenes from propargylic alcohols[24] prompted us to use a similar strategy to detect the formation of ruthenium vinyl carbenes through CAM, considering that propargylic alcohols proved to be competent substrates for tandem reactions involving CAM processes.[12c] Thus, we prepared complex **7** by combining the readily available tetramer $[Cp^*RuCl]_4$ and 1-(1-propynyl)cyclohexanol (Scheme 2). This complex was then treated with 1 equiv. of trimethylsilyldiazomethane, causing an instantaneous color change from deep purple to dark brown/green, and the crude mixture was analyzed by NMR.

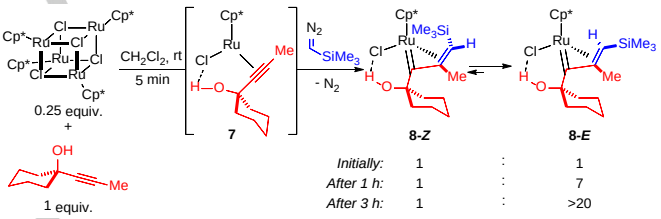

Scheme 2. Preparation of a Ru η^3-vinylcarbene by CAM.

To our initial surprise, the clean formation of two isomeric carbenic species, as revealed by the appearance of two strongly deshielded resonances at 316.3 ppm and 312.1 ppm in ^{13}C-NMR, was observed after 10 min of reaction at room temperature in a 1:1 ratio, which after 2-3 h evolved to just one single isomer (see Supporting Information for details). NOESY experiments allowed us to attribute the generation of these two species to the isomerization of the kinetically favored **8-*Z*** to the more thermodynamically stable **8-*E*** ruthenium vinyl carbene, which was previously accounted by DFT calculations in our group.[25] After total isomerization, vinyl carbene **8-*E*** proved to be relatively stable in solution for several days, which allowed its full characterization by NMR techniques (Table 1). A series of statements can be inferred from these data:

i. Neither ^{1}H-NMR signals of the monosubstituted carbene derived from decomposition of trimethylsilyldiazomethane[26] nor evidences of binuclear complexes of type **6** (Figure 2) were observed, which indicates just the formation of a disubstituted donor-donor carbene through a rapid CAM.

ii. Even though we started from an internal alkyne, the CAM step shows a high regioselectivity forming only the compound with the carbene adjacent to the carbon bearing the hydroxyl group as shown by its deshielding in ^{13}C-NMR (89.7 ppm vs. 69.0 ppm in the starting propargylic alcohol). Moreover, the ^{1}H-NMR low-field shift of the OH from 1.97 ppm to 3.30 ppm indicates an interligand hydrogen bond between the hydroxyl group and the chloride ligand,[24b,27] which may be responsible, together with the different steric hindrance at both sides of the alkyne, of the regioselectivity control.

iii. The shielding of both ^{1}H-NMR and ^{13}C-NMR signals of the alkene moiety totally agrees with the only ruthenium η^3-vinylcarbene reported to date in literature (**5** in Figure 2).[28] Thus, vinylic hydrogen 5 and carbon 5 showed higher-field resonance signals than typically found in uncoordinated olefins,[26a] 2.78 ppm and 62.3 ppm, respectively, as well as the quaternary carbon 6, at 87.4 ppm (Table 1).

iv. The ruthenium atom becomes tetrasubstituted and, therefore, chiral as suggested by the appearance of diastereotopic carbons in the cyclohexane ring (4, Table 1) as shown in the ^{13}C-NMR spectrum.

Table 1. Spectroscopic data for ruthenium vinyl carbene **8-*E***.

^{1}H-NMR

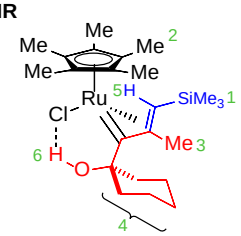

^{13}C-NMR

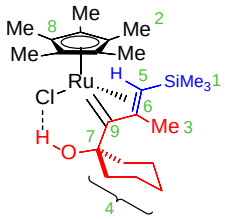

^{1}H-NMR	δ (ppm)	^{13}C-NMR	δ (ppm)
1	0.20	1	0.7
2	1.75	2	11.3
3	1.88	3	16.2
4	1.42-1.95	4	21.0, 21.8, 26.0, 29.8, 32.7
5	2.78	5	62.3
6	3.30	6	87.4
		7	89.7
		8	99.7
		9	316.3

DFT description of a Cp*RuCl η^3-vinylcarbene

In order to compare the high reactivity of Cp/Cp*RuCl η^3-vinylcarbenes arising from the combination of diazocompounds and alkynes in CAM processes[12-15,17-18] with the unreactive ruthenium η^3-vinylcarbene **5** (Figure 2), we performed a thorough geometrical/electronic description of the former species using DFT calculations. Accordingly, η^3 coordination induces an out-of-plane bending of the Ru-C1-C2-C3 fragment of roughly 18° (Figure 3) which exposes preferentially one side of the carbene towards a potential nucleophilic attack.

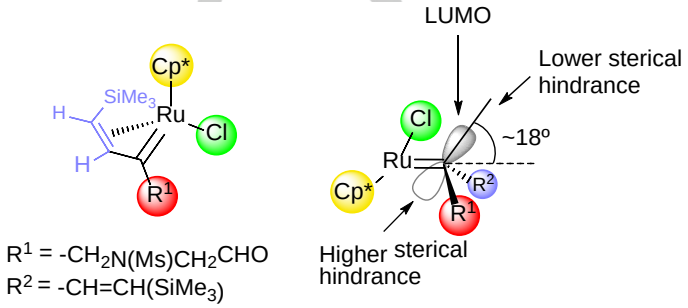

Figure 3. Structural description of a Cp*RuCl η^3-vinylcarbene by DFT modeling.

Unlike typical Grubbs-type vinyl carbenes, DFT calculations show that Cp*RuCl η^3-vinylcarbenes are significantly more stable than its η^1 counterpart (Figure 4), probably due to a combination of geometrical restrictions imposed by the piano-stool disposition of the ligands, the intramolecular steric repulsion between alkyl chains in the donor-donor carbene and the increased stability of an 18 e$^-$ complex as compared to an unsaturated 16 e$^-$ complex. At the same time, η^3-coordination saturates the metal and would prevent (or seriously hamper) further evolution through metathesis with other olefins or alkynes.[22,29]

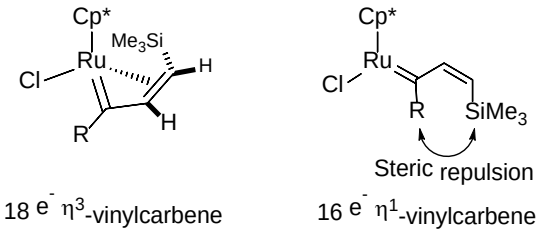

Figure 4. Steric and electronic stabilization of Cp*RuCl η^3-vinylcarbene *vs.* η^1-vinylcarbene.

Having established the unique geometrical and electronic properties of Cp*RuCl η^3-vinylcarbenes we now focus our attention on their divergent reactivity towards alkynals with the

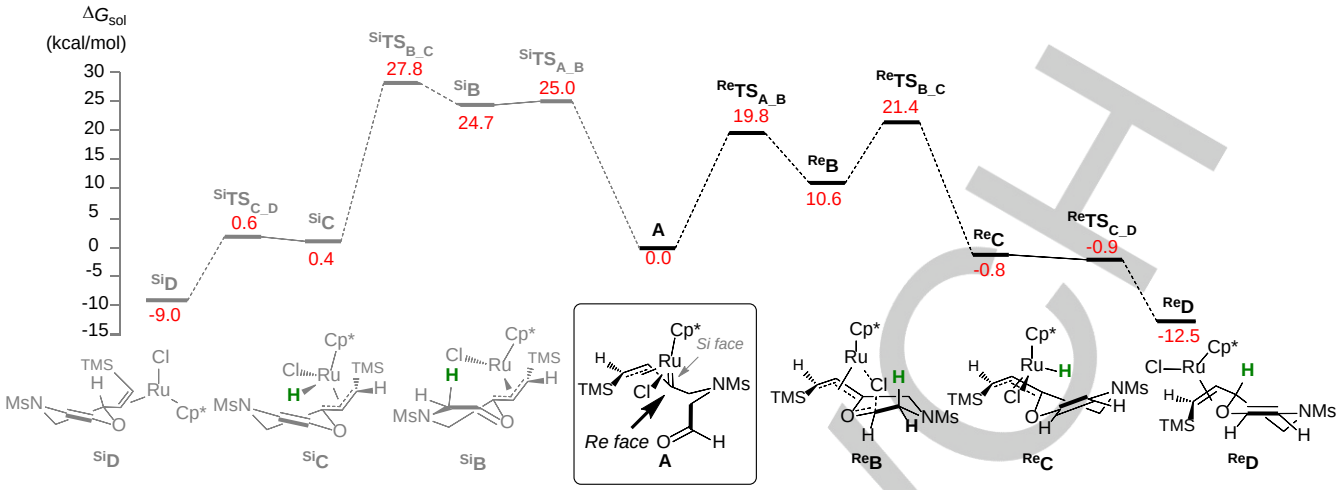

Figure 5. Free energy profile for the formation of vinyl dihydrooxazines through ylide formation. Note: For the sake of simplicity, TMS = $SiMe_3$.

elucidation of the mechanistic pathways that lead to vinyl dihydrooxazines **2** or vinyl epoxypyrrolidines **3** depending on the aza-alkynal **1** used (Scheme 1).

Ylide formation vs. (2+1) cycloaddition with α-unsubstituted aza-alkynals. The non-innocent role of Cl ligand.

First, the mechanism for the formation of vinyl dihydrooxazine from aza-alkynal **1a** was examined. The two possible pathways arising from the nucleophilic addition of the carbonyl group to both sterically differentiated faces of the initially formed [Cp*RuCl] η^3-vinylcarbene **A** were computed (Figure 5).[30] Interestingly, the nucleophilic addition of the carbonyl to the ruthenium carbene through the *Re* face is significantly more favorable than the addition through the *Si* face (^{Re}**TS**$_{A\_B}$ vs. ^{Si}**TS**$_{A\_B}$). Moreover, ylide intermediate ^{Re}**B** is 14.1 kcal/mol more stable than ylide ^{Si}**B**. Such remarkable difference in energy cannot be only attributed to an increased steric hindrance through the *Si* face of the carbene; thus, a closer examination of the structures of both transition states and intermediates revealed an unexpected contribution of the Cl ligand (Figure 6): i) in the **A**→^{Re}**B** step, the Ru-Cl bond distance increases by 0.17 Å; however, in the **A**→^{Si}**B** step, an elongation of only 0.05 Å is observed; ii) the $C_{aldehyde\text{-}Cl}$ distance in ^{Re}**B** is 1.89 Å, which is well below the sum of the van der Walls radii of both atoms (3.52 Å) and close to a standard C-Cl single bond (1.75-1.85 Å); iii) the carbonyl carbon in ^{Re}**B** clearly experiments a deviation from planarity, which indicates a partial sp^3 rehybridization due to the proximity of the Cl ligand. All these evidences suggest that the chloride ligand acts as a Lewis-base cocatalyst by a) facilitating the nucleophilic addition to the vinyl carbene, b) stabilizing polarized intermediates (ion pair) and c) modulating the electron density at the Ru(II) center by partial dissociation.

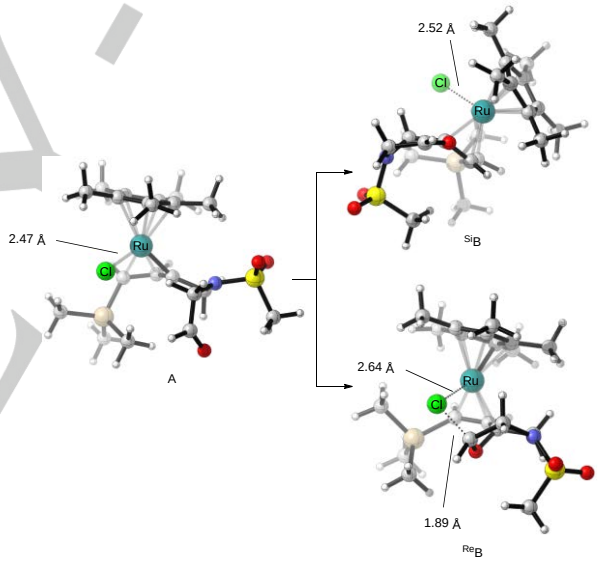

Figure 6. Optimized structures for ruthenium vinyl carbene **A** and ylide intermediates ^{Si}**B** and ^{Re}**B**.

Ylide **B** would subsequently evolve through **TS**$_{B\_C}$ via an intramolecular 1,5-hydrogen shift of the pseudo-axial proton in *syn* disposition respect to the Cp*RuCl fragment (highlighted in green in Figure 5) followed by an almost barrierless reductive elimination of the formed ruthenium hydride species **C** to afford the coordinated vinyl dihydrooxazine **D**. Once again, the non-innocent chloride ligand is responsible for the more favorable hydrogen shift through the *Re* face than through the *Si* face ($\Delta\Delta G^{\ddagger}$ ^{Si}**TS**$_{B\_C}$ vs. ^{Re}**TS**$_{B\_C}$ = 6.4 kcal/mol) by creating a coordination vacant on the ruthenium due its partial dissociation in intermediate ^{Re}**B**.[31]

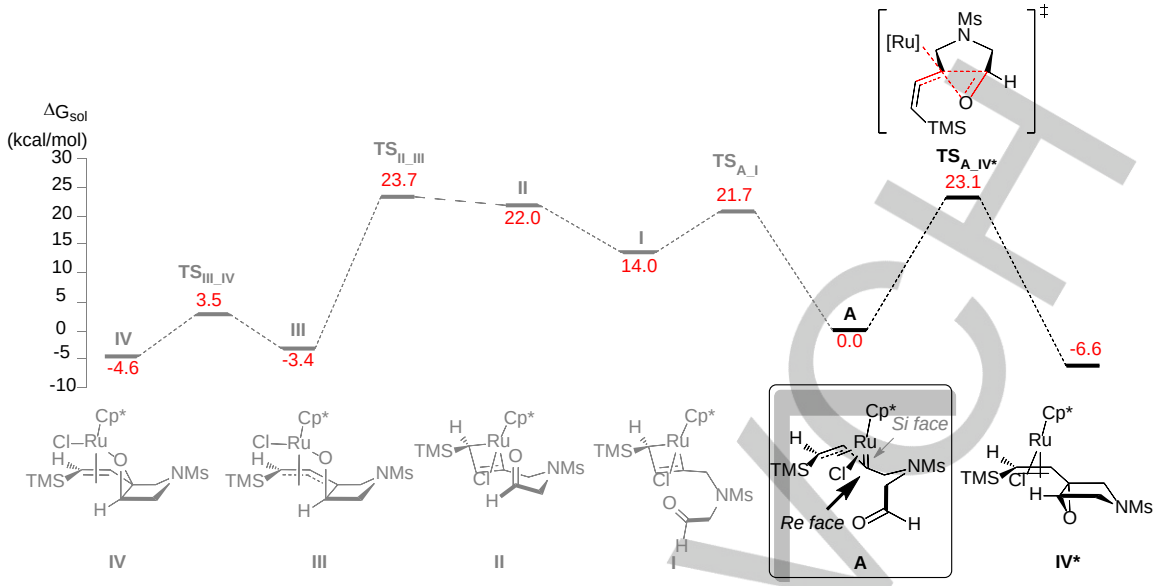

Figure 7. Free energy profile for the formation of vinyl epoxypyrrolidines. Note: For the sake of simplicity, TMS = $SiMe_3$.

The mechanism of the competitive vinyl epoxypyrrolidine formation was subsequently analyzed. After an extensive examination, two reaction pathways that lead to the formation of epoxypyrrolidines were identified, being both only operative through the less sterically hindered *Re* face of the carbene (Figure 6).[32]

The first mechanism examined (Figure 7, grey pathway) involves an endergonic electrocyclization of the ruthenium vinyl carbene **A** to the ruthenacyclobutene **I**. Then, after a conformational rearrangement of the alkyl chain (**I**→**II**), an almost barrierless 1,2-migratory insertion ($\Delta G^{\ddagger}$(**TS_{II_III}**) = 1.7 kcal/mol) of the carbonyl group into the Ru-C_{sp2} bond of the ruthenacyclobutene irreversibly affords the oxaruthenacycle **III**. Finally, intermediate **III** undergoes a facile reductive elimination to give the observed epoxypyrrolidine coordinated to the Cp*RuCl fragment.

Alternatively, vinyl carbene **A** was also found to directly evolve to epoxypyrrolidine **IV*** through an irreversible and concerted (2+1) cycloaddition ($\Delta G^{\ddagger}$(**TS_{A_IV*}**) = 23.1 kcal/mol, Figure 7, black pathway). To the best of our knowledge, such reaction pathway has never been considered in literature concerning (2+1) cycloadditions of polarized C=X bonds (X = heteroatom).

Even though the latter mechanism is only slightly lower in energy than the former and, therefore, we cannot unequivocally determine the precise mechanism for the formation of epoxypyrrolidines, comparing the pathways shown in Figures 5 and 6, we can conclude that vinyl carbene **A**, derived from an α-unsubstituted alkynal, preferentially evolves to dihydrooxazine **^{Re}D** ($\Delta\Delta G^{\ddagger}$ **TS_{A_IV*}** vs. **$^{Re}TS_{B\_C}$** = 1.7 kcal/mol), which is in accord with the experimental result.

The case of α-monosubstituted alkynals

The chemoselective cyclization of α-monosubstituted alkynals was analyzed next. To this end, (*S*)-configured alkynal **1b** (a *L*-alanine derivative) was selected as the model substrate. It is important to note that, given the chiral nature of alkynal **1b** and the chiral-at-metal ruthenium complexes two possible diastereoisomers arise upon coordination of the alkyne to the metal center (***i*** and ***ii*** complexes, Figure 8). This fact was taken into consideration not only for the study of chemoselectivity but also for the diastereoselectivity of the epoxy-annulation reaction.

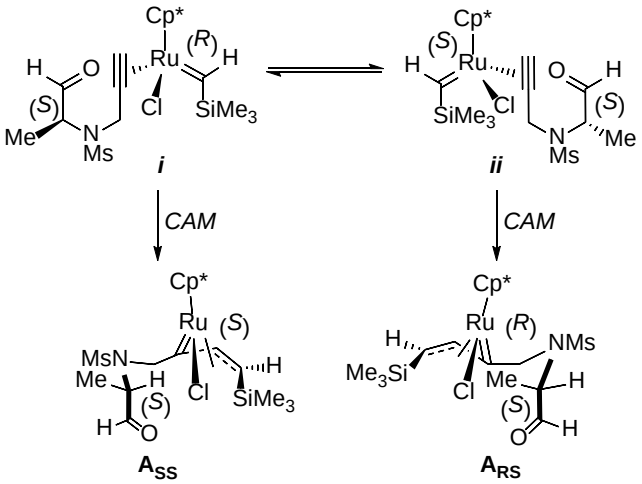

Figure 8. Two possible scenarios arise upon coordination of chiral alkynal **1b** to a prochiral ruthenium complex.

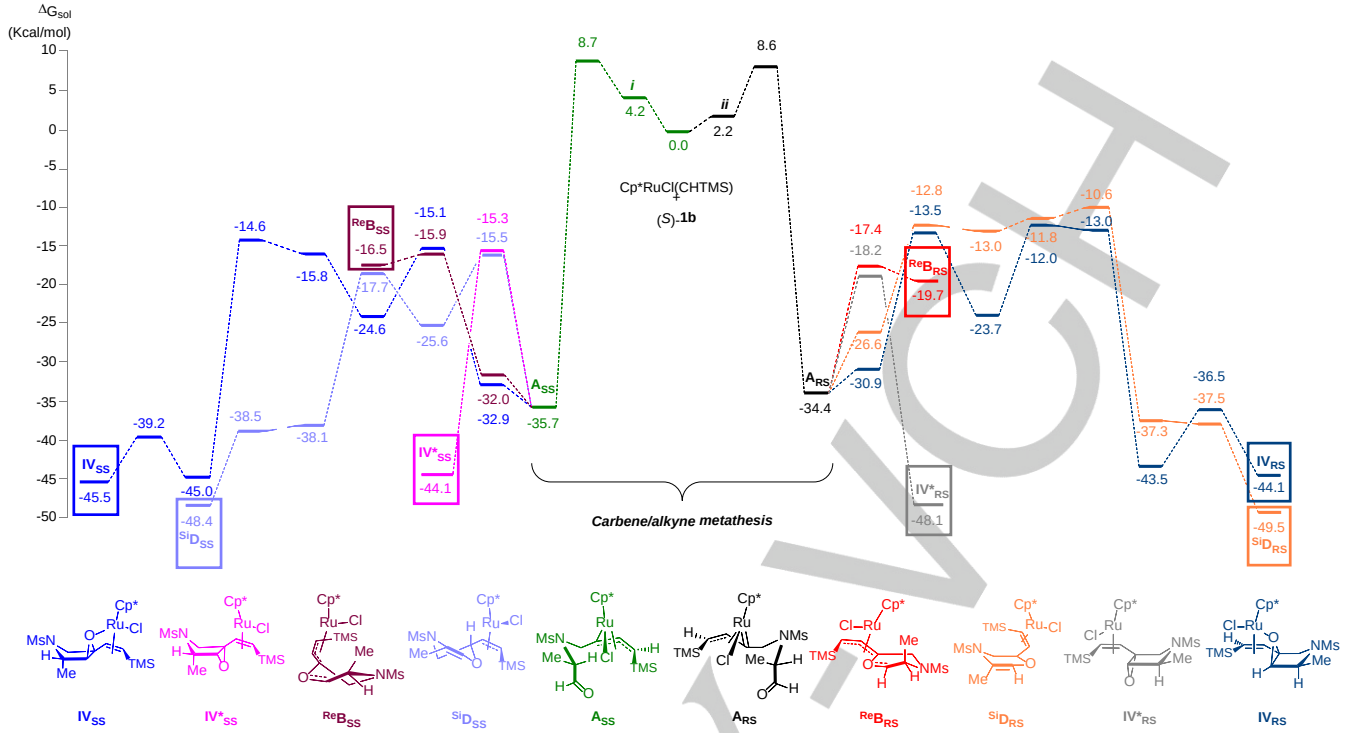

Figure 9. Free energy profile for the chemoselective cyclization of α-monosubstituted alkynals. Vinyl dihydrooxazine vs. Vinyl epoxypyrrolidine. Note: For the sake of simplicity, TMS = $SiMe_3$.

All possible routes for the cyclization of alkynal **1b** (ylide formation through the *Si* and *Re* faces of the carbene in complexes **A**$_{SS}$ and **A**$_{RS}$, concerted/stepwise (2+1) cycloadditions to epoxypyrrolidines and *Z* to *E* isomerizations of the vinyl moiety) have been considered, showing only the lowest energy pathways in Figure 9 leading either to dihydrooxazine or epoxypyrrolidine products (for other less relevant reaction pathways see Supporting Information).

The reaction starts with the formation of the two diastereomeric ruthenium carbenes ***i*** and ***ii*** ($\Delta\Delta G^{o}$ (***i***, ***ii***) = 2.0 kcal/mol) by coordination of alkynal **1b** to the ruthenium carbene complex, followed by an irreversible CAM reaction through very similar activation barriers ($\Delta G^{\ddagger}$ = 8.7 and 8.6 kcal/mol for **TS**$_{i\_ASS}$ and **TS**$_{ii\_ARS}$, respectively) to afford ruthenium vinyl carbenes **A**$_{SS}$ and **A**$_{RS}$. From this point, both diastereomeric vinyl carbene species follow different reaction pathways.

On the one hand, vinyl carbene **A**$_{RS}$ preferentially evolves to epoxypyrrolidine **IV*$_{RS}$** through a concerted (2+1) cycloaddition (grey pathway, $\Delta\Delta G^{\ddagger}$ = 16.2 kcal/mol. Figure 9) rather than to dihydrooxazine by nucleophilic attack of the carbonyl group to the vinyl carbene through the *Re* face ($\Delta\Delta G^{\ddagger}$ (**TSA**$_{RS}$_^{Re}**B**$_{RS}$, **TSA**$_{RS}$_**IV*$_{RS}$**) = 0.8 kcal/mol) which reversibly provides ylide ^{Re}**B**$_{RS}$ (red pathway), which cannot further evolve due to the lack of a hydrogen atom at α position with a *syn* disposition respect to the Cp*RuCl fragment (1,5-migration is not possible). In addition, the presence of this methyl group in ^{Re}**B**$_{RS}$ precludes the assistance of the chloride ligand in the nucleophilic attack due to steric hindrance, thus, increasing the activation energy for the nucleophilic attack (Lewis catalysis Off). The alternative for the dihydrooxazine formation, nucleophilic attack of the carbonyl through the *Si* face (orange pathway), is not feasible either ($\Delta\Delta G^{\ddagger}$ = 7.6 kcal/mol above the concerted (2+1) cycloaddition, Lewis catalysis Off). Remarkably, the stepwise (2+1) cycloaddition that involves the electrocyclization of the vinyl carbene **A**$_{RS}$ to the ruthenacyclobutene (indigo pathway) is significantly higher in energy respect to the concerted route ($\Delta\Delta G^{\ddagger}$ = 6.2 kcal/mol).

On the other hand, the fate of vinyl carbene **A**$_{SS}$ is not so clear. The pathway to dihydrooxazine ^{Si}**D**$_{SS}$ by nucleophilic attack of the carbonyl group to the *Si* face of the vinyl carbene, assisted by the chloride ligand (chloride Lewis catalysis On), and subsequent 1,5-hydrogen migration (pseudo-axial hydrogen in *syn* disposition) are possible (clear blue pathway) and competitive with the concerted (2+1) cycloaddition (pink pathway) to epoxypyrrolidine **IV*$_{SS}$** ($\Delta\Delta G^{\ddagger}$ (**TSA**$_{SS}$_**IV*$_{SS}$**, **TSA**$_{SS}$_^{Si}**D**$_{SS}$) = 0.2 kcal/mol). As for the diastereoisomer **A**$_{RS}$, pathways to dihydrooxazine ^{Re}**B**$_{SS}$ by nucleophilic attack of the carbonyl through the *Re* face (brown pathway), would place the methyl group *syn* to the Cp*RuCl fragment, precluding its evolution to dihydrooxazines, while stepwise (2+1) cycloaddition to epoxypyrrolidines (dark blue pathway) is higher in energy.

In order to determine the relative final distribution of products from the potential energy surface shown in Figure 9, we performed kinetic Monte-Carlo (KMC) simulations[25,33] from the α-monosubstituted alkynal (*S*)-**1b** and Cp*RuCl(CHSiMe$_3$) (Figure 10). According to this simulation, after a rapid CAM (2 x 10^{-6} s), vinyl ruthenium carbenes $\mathbf{A_{RS}}$ and $\mathbf{A_{SS}}$ are formed in a 57:43 ratio, respectively. As previously explained, intermediate $\mathbf{A_{RS}}$ exclusively affords the vinyl epoxypyrrolidine **IV*$_{RS}$**, with a 1*R*,4*S*,5*S* configuration of the stereocenters, in a 57% yield, being other alternative reaction pathways negligible. On the other hand, vinyl ruthenium carbene $\mathbf{A_{SS}}$ yielded, through two competitive processes which are very close in energy, the dihydrooxazine $\mathbf{^{Si}D_{SS}}$ in a 23% yield and the epoxypyrrolidine **IV*$_{SS}$**, with a 1*S*,4*S*,5*R* configuration of the stereocenters, in a 17% yield.

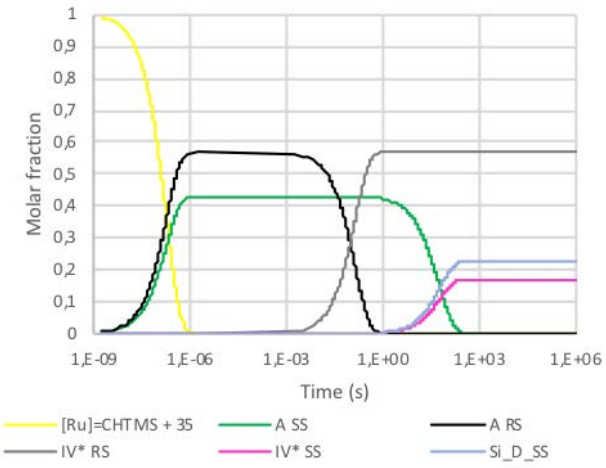

Figure 10. KMC simulation for the evolution of alkynal (*S*)-**1b** as a function of molar fraction and time.

Theoretical and experimental results are in reasonably good agreement not only identifying the major product, but, remarkably, in the ratio and absolute configuration of the two diastereoisomeric epoxypyrrolidines obtained as shown in Scheme 3 and Figure 11.[34] According to the calculated reaction profile, the epoxypyrrolidine should be obtained in a 74% yield as a 3.3:1 mixture of diastereomers and the dihydrooxazine in a 23% yield. This prediction is in a reasonably good agreement with the experimental results (50% isolated yield of epoxypyrrolidine in a 2.3:1 ratio of diastereomers). Our results suggest that the diastereoselectivity observed in the cyclization of α-monosubstituted alkynals cannot be attributed to any steric/electronic differentiation in the starting material, but to the partial destruction of one of the diastereoisomeric vinyl carbene intermediates ($\mathbf{A_{SS}}$ in the present case), which also explains the lower reaction yields obtained with these substrates as compared with α-disubstituted alkynals.

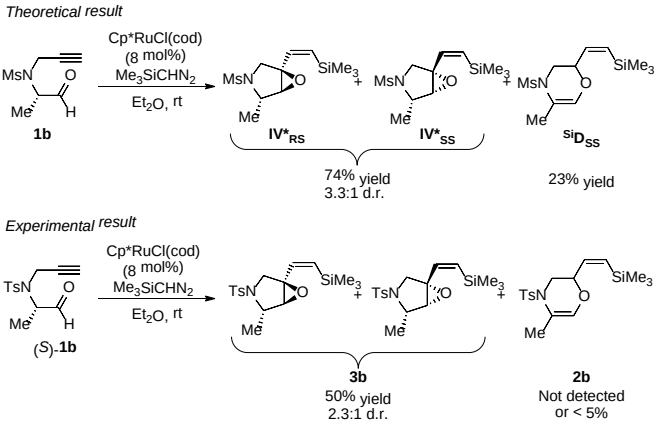

Scheme 3. Comparison between the theoretical and the experimental outcome of the cyclization of α-substituted alkynals.

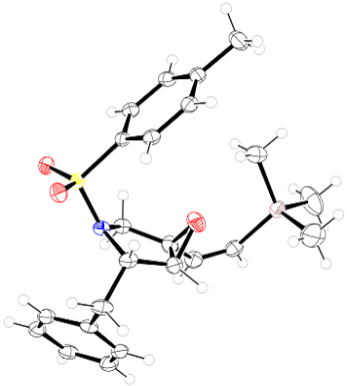

Figure 11. X-ray diffraction analysis of an analogue of epoxypyrrolidine **3b** (benzyl- instead of methyl-substituted epoxypyrrolidine).

All experimental and computational data presented in the previous sections allowed us to propose the mechanistic rationale depicted in Figure 12 for the cyclization of alkynals. First, the Cp*RuCl(cod) complex easily loses its cod ligand in the presence of trimethylsilyldiazomethane and the alkynal to afford intermediate ***i*/*ii***. After a fast and concerted CAM reaction, a distorted η^3-vinyl carbene **A** is formed irreversibly. At this stage, the mechanism bifurcates depending on the presence/absence of substituents at α position to the carbonyl group. With α-unsubstituted alkynals, vinyl carbene **A** preferentially evolves through a reversible nucleophilic attack to afford ylide **B**. This nucleophilic attack must occur through the face that places the carbonyl group close to the chloride ligand, thus benefiting from a Lewis-base assistance. Then, a metal-assisted 1,5-hydrogen migration gives rise to species **C**, which undergoes a rapid reductive elimination to afford the observed dihydropyran/dihydrooxazine.

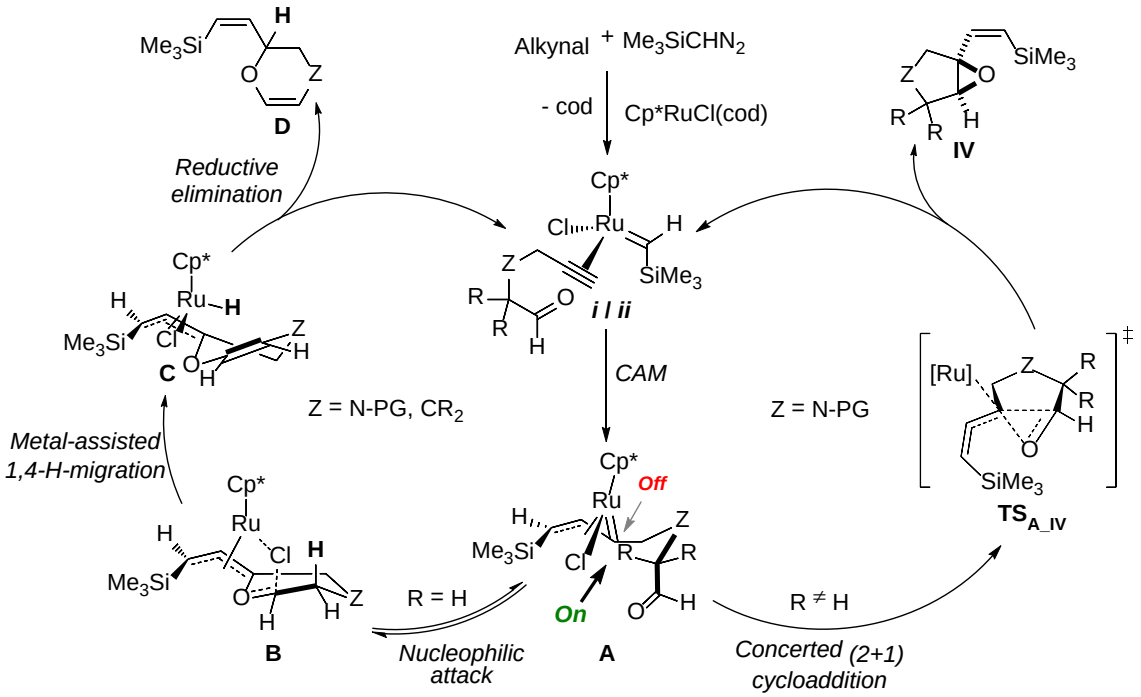

Figure 12. General mechanistic proposal for the cyclization of alkynals.

Alternatively, vinyl carbene **A**, derived from an α-substituted alkynal, preferentially evolves through a concerted (2+1) cycloaddition (**TS**$_{A\_IV}$) to directly give epoxypyrrolidines.

Conclusion

To conclude, a combined experimental and computational study has been performed in order to shed some light on the peculiarities of half-sandwich ruthenium vinyl carbenes derived from a carbene/alkyne metathesis process. According to our results, the piano-stool arrangement of Cp*RuCl-vinylcarbenes favors a η^3-coordination mode which induces a deformation from planarity of the ruthenium carbene. Such distortion seems to increase the reactivity of the ruthenium vinyl carbene. At the same time, the presence of the chloride ligand in an appropriate disposition acts as a Lewis base cocatalyst and promotes nucleophilic attacks to the ruthenium vinyl carbene. The combination of these effects are directly related to the divergent behavior of these species with α-unsubstituted and α-substituted alkynals. While the absence of substitution at α position enables ylide formation and subsequent 1,5-hydrogen migration/reductive elimination to dihydrooxazines, substitution at α position hinders the latter pathway and decreases the energetic barrier for an unconventional concerted (2+1) cycloaddition between the metal carbene and the carbonyl group to yield epoxypyrrolidines. We anticipate that the results presented herein can be applied to the development of new divergent transformations.

Experimental Section

Experimental part including characterization data, computational details, optimized geometric parameters for all calculated structures and non-active reaction pathways.

Acknowledgements

This work has received financial support from MINECO (project CTQ2017-87939R and ORFEO-CINQA network CTQ2016-81797-REDC and RED2018-102387-T), the Xunta de Galicia (project ED431C 2018/04 and Centro singular de investigación de Galicia accreditation 2016-2019, ED431G/09) and the European Union (European Regional Development Fund – ERDF). D.P. thanks MEC for a predoctoral FPU fellowship (FPU15/02132). We are also grateful to the CESGA (Xunta de Galicia) for computational time.

Keywords: carbenes • cycloadditions • metathesis • ruthenium • ylides

[1] a) A. H. Hoveyda, A. R. Zhugralin, *Nature* **2007**, *450*, 243-251; b) G. C. Vougioukalakis, R. H. Grubbs, *Chem. Rev.* **2010**, *110*, 1746-1787.

[2] a) H. Lebel, J.-F. Marcoux, C. Molinaro, A. B. Charette, *Chem. Rev.* **2003**, *103*, 977-1050; b) H. M. L. Davies, E. G. Antoulinakis, in "Intermolecular Metal‐Catalyzed Carbenoid Cyclopropanations", *Org. Reac.*, **2004**.

[3] A. Padwa, S. F. Hornbuckle, *Chem. Rev.* **1991**, *91*, 263-309.

[4] Y. Xia, D. Qiu, J. Wang, *Chem. Rev.* **2017**, *117*, 13810-13889.

[5] a) H. M. L. Davies, M. Pelphrey Phillip, in "Intermolecular C–H Insertions of Carbenoids", *Org. Reac.*, **2004**; b) H. M. L. Davies, J. R. Manning, *Nature* **2008**, *451*, 417-424; c) M. P. Doyle, R. Duffy, M. Ratnikov, L. Zhou, *Chem. Rev.* **2010**, *110*, 704-724; d) T. Yakura, H. Nambu, *Tetrahedron Lett.* **2018**, *59*, 188-202.

[6] a) A. Padwa, M. D. Weingarten, *Chem. Rev.* **1996**, *96*, 223-270; b) A. Padwa, *Chem. Soc. Rev.* **2009**, *38*, 3072-3081; c) A. Fürstner, *Chem. Soc. Rev.* **2009**, *38*, 3208-3221.

[7] a) Y. Ni, J. Montgomery, *J. Am. Chem. Soc.* **2004**, *126*, 11162-11163; b) Y. Ni, J. Montgomery, *J. Am. Chem. Soc.* **2006**, *128*, 2609-2614; c) S. Jansone-Popova, J. A. May, *J. Am. Chem. Soc.* **2012**, *134*, 17877-17880; d) Y. Shi, V. Gevorgyan, *Org. Lett.* **2013**, *15*, 5394-5396; e) Y. Zheng, J. Mao, Y. Weng, X. Zhang, X. Xu, *Org. Lett.* **2015**, *17*, 5638-5641; f) Ò. Torres, T. Parella, M. Solà, A. Roglans, A. Pla-Quintana, *Chem. Eur. J.* **2015**, *21*, 16240-16245; g) P. Q. Le, J. A. May, *J. Am. Chem. Soc.* **2015**, *137*, 12219-12222; h) R. Yao, G. Rong, B. Yan, L. Qiu, X. Xu, *ACS Catalysis* **2016**, *6*, 1024-1027; i) X. Wang, Y. Zhou, L. Qiu, R. Yao, Y. Zheng, C. Zhang, X. Bao, X. Xu, *Adv. Synth. Catal.* **2016**, *358*, 1571-1576; j) H. Qiu, Y. Deng, K. O. Marichev, M. P. Doyle, *J. Org. Chem.* **2017**, *82*, 1584-1590; k) P.-A. Chen, K. Setthakarn, J. A. May, *ACS Catalysis* **2017**, *7*, 6155-6161; l) Y. Zheng, M. Bao, R. Yao, L. Qiu, X. Xu, *Chem. Commun.* **2018**, *54*, 350-353.

[8] a) A. Padwa, *Molecules* **2001**, *6*, 1-12; b) A. Padwa, *J. Organomet. Chem.* **2001**, *617-618*, 3-16.

[9] a) Y. Qian, C. S. Shanahan, M. P. Doyle, *Eur. J. Org. Chem.* **2013**, *2013*, 6032-6037; b) C. Pei, C. Zhang, Y. Qian, X. Xu, *Org. Biomol. Chem.* **2018**, *16*, 8677-8685.

[10] a) S. T. Diver, A. J. Giessert, *Chem. Rev.* **2004**, *104*, 1317-1382; b) H. Villar, M. Frings, C. Bolm, *Chem. Soc. Rev.* **2007**, *36*, 55-66; c) C. Fischmeister, C. Bruneau, *Beilstein J. Org. Chem.* **2011**, *7*, 156-166.

[11] a) C. Vovard-Le Bray, S. Dérien, P. H. Dixneuf, *C. R. Chim.* **2010**, *13*, 292-303; b) D. Padín, J. A. Varela, C. Saá, in "Vinyl Ruthenium Carbenes: Valuable Intermediates in Catalysis", *New Horizons of Process Chemistry: Scalable Reactions and Technologies* (Eds.: K. Tomioka, T. Shioiri, H. Sajiki), Springer Singapore, **2017**, pp. 89-102.

[12] a) J. Le Paih, S. Dérien, I. Özdemir, P. H. Dixneuf, *J. Am. Chem. Soc.* **2000**, *122*, 7400-7401; b) C. Vovard‐Le Bray, S. Dérien, H. Dixneuf Pierre *Angew. Chem. Int. Ed.* **2009**, *48*, 1439-1442; *Angew. Chem.* **2009**, *121*, 1467-1470; c) J. L. Paih, C. V.-L. Bray, S. Dérien, P. H. Dixneuf, *J. Am. Chem. Soc.* **2010**, *132*, 7391-7397.

[13] a) F. Monnier, D. Castillo, S. Dérien, L. Toupet, H. Dixneuf Pierre, *Angew. Chem. Int. Ed.* **2003**, *42*, 5474-5477; *Angew. Chem.* **2003**, *115*, 5632-5635; b) M. Eckert, F. Monnier, G. T. Shchetnikov, I. D. Titanyuk, S. N. Osipov, L. Toupet, S. Dérien, P. H. Dixneuf, *Org. Lett.* **2005**, *7*, 3741-3743; c) F. Monnier, C. Vovard-Le Bray, D. Castillo, V. Aubert, S. Dérien, P. H. Dixneuf, L. Toupet, A. Ienco, C. Mealli, *J. Am. Chem. Soc.* **2007**, *129*, 6037-6049; d) C. Vovard-Le Bray, S. Dérien, P. H. Dixneuf, M. Murakami, *Synlett* **2008**, *2008*, 193-196; e) M. Eckert, S. Moulin, F. Monnier, D. Titanyuk Igor, N. Osipov Sergey, T. Roisnel, S. Dérien, H. Dixneuf Pierre, *Chem. Eur. J.* **2011**, *17*, 9456-9462.

[14] F. Cambeiro, S. López, A. Varela Jesús, C. Saá, *Angew. Chem. Int. Ed.* **2012**, *51*, 723-727; *Angew. Chem.* **2012**, *124*, 747-751.

[15] C. González‐Rodríguez, R. Suárez José, A. Varela Jesús, C. Saá, *Angew. Chem. Int. Ed.* **2015**, *54*, 2724-2728; *Angew. Chem.* **2015**, *127*, 2762-2766.

[16] a) D.-Y. Zhang, F.-L. Zhu, Y.-H. Wang, X.-H. Hu, S. Chen, C.-J. Hou, X.-P. Hu, *Chem. Commun.* **2014**, *50*, 14459-14462; b) L. Xia, R. Lee Yong, *Eur. J. Org. Chem.* **2014**, *2014*, 3430-3442.

[17] F. Cambeiro, S. López, J. A. Varela, C. Saá, *Angew. Chem. Int. Ed.* **2014**, *53*, 5959-5963; *Angew. Chem.* **2014**, *126*, 6069-6073.

[18] D. Padín, F. Cambeiro, M. Fañanás-Mastral, J. A. Varela, C. Saá, *ACS Catalysis* **2017**, *7*, 992-996.

[19] a) See Supp. Info. for details. W. J. Hehre, R. Ditchfield, J. A. Pople; *J. Chem. Phys.* **1972**, *56*, 2257-2261; b) P. C. Hariharan, J. A. Pople, *Theoretica chimica acta* **1973**, *28*, 213-222; c) A. D. McLean, G. S. Chandler, *J. Chem. Phys.* **1980**, *72*, 5639-5648; d) R. Krishnan, J. S. Binkley, R. Seeger, J. A. Pople, *J. Chem. Phys.* **1980**, *72*, 650-654; e) P. J. Hay, W. R. Wadt, *J. Chem. Phys.* **1985**, *82*, 270-283; f) P. J. Hay, W. R. Wadt, *J. Chem. Phys.* **1985**, *82*, 299-310; g) K. A. Peterson, D. Figgen, M. Dolg, H. Stoll, *J. Chem. Phys.* **2007**, *126*, 124101; h) J.-D. Chai, M. Head-Gordon, *Phys. Chem. Chem. Phys.* **2008**, *10*, 6615-6620; i) J.-D. Chai, M. Head-Gordon, *J. Chem. Phys.* **2008**, *128*, 084106; j) A. V. Marenich, C. J. Cramer, D. G. Truhlar, *J. Phys. Chem. B* **2009**, *113*, 6378-6396.

[20] M. J. Frisch, G. W. Trucks, H. B. Schlegel, G. E. Scuseria, M. A. Robb, J. R. Cheeseman, G. Scalmani, V. Barone, B. Mennucci, G. A. Petersson, H. Nakatsuji, M. Caricato, X. Li, H. P. Hratchian, A. F. Izmaylov, J. Bloino, G. Zheng, J. L. Sonnenberg, M. Hada, M. Ehara, K. Toyota, R. Fukuda, J. Hasegawa, M. Ishida, T. Nakajima, Y. Honda, O. Kitao, H. Nakai, T. Vreven, J. A. Montgomery, Jr., J. E. Peralta, F. Ogliaro, M. Bearpark, J. J. Heyd, E. Brothers, K. N. Kudin, V. N. Staroverov, T. Keith, R. Kobayashi, J. Normand, K. Raghavachari, A. Rendell, J. C. Burant, S. S. Iyengar, J. Tomasi, M. Cossi, N. Rega, J. M. Millam, M. Klene, J. E. Knox, J. B. Cross, V. Bakken, C. Adamo, J. Jaramillo, R. Gomperts, R. E. Stratmann, O. Yazyev, A. J. Austin, R. Cammi, C. Pomelli, J. W. Ochterski, R. L. Martin, K. Morokuma, V. G. Zakrzewski, G. A. Voth, P. Salvador, J. J. Dannenberg, S. Dapprich, A. D. Daniels, O. Farkas, J. B. Foresman, J. V. Ortiz, J. Cioslowski, and D. J. Fox, *Gaussian 09*, revision E.01, Gaussian Inc., Wallingford CT, **2013**.

[21] a) S. T. Nguyen, L. K. Johnson, R. H. Grubbs, J. W. Ziller, *J. Am. Chem. Soc.* **1992**, *114*, 3974-3975; b) M. R. Gagne, R. H. Grubbs, J. Feldman, J. W. Ziller, *Organometallics* **1992**, *11*, 3933-3935; c) S. T. Diver, *Coord. Chem. Rev.* **2007**, *251*, 671-701; d) S. T. Nguyen, T. M. Trnka, *Handbook of Metathesis* **2008**.

[22] T. M. Trnka, M. W. Day, R. H. Grubbs, *Organometallics* **2001**, *20*, 3845-3847.

[23] J. J. Lippstreu, B. F. Straub, *J. Am. Chem. Soc.* **2005**, *127*, 7444-7457.

[24] a) M. Leutzsch, L. M. Wolf, P. Gupta, M. Fuchs, W. Thiel, C. Farès, A. Fürstner, *Angew. Chem. Int. Ed.* **2015**, *54*, 12431-12436; *Angew. Chem.* **2015**, *127*, 12608-12613; b) S. M. Rummelt, K. Radkowski, D.-A. Roşca, A. Fürstner, *J. Am. Chem. Soc.* **2015**, *137*, 5506-5519; c) D.-A. Roşca, K. Radkowski, L. M. Wolf, M. Wagh, R. Goddard, W. Thiel, A. Fürstner, *J. Am. Chem. Soc.* **2017**, *139*, 2443-2455; d) A. Guthertz, M. Leutzsch, L. M. Wolf, P. Gupta, S. M. Rummelt, R. Goddard, C. Farès, W. Thiel, A. Fürstner, *J. Am. Chem. Soc.* **2018**, *140*, 3156-3169; e) T. Biberger, C. P. Gordon, M. Leutzsch, S. Peil, A. Guthertz, C. Copéret, A. Fürstner, *Angew. Chem. Int. Ed.* **2019**, *58*, 8845-8850; *Angew. Chem.* **2019**, *131*, 8937-8942; f) A. Fürstner, *J. Am. Chem. Soc.* **2019**, *141*, 11-24; g) S. Peil, A. Guthertz, T. Biberger, A. Fürstner, *Angew. Chem. Int. Ed.* **2019**, *58*, 8851-8856, *Angew. Chem.* **2019**, 131, 8943-8948.

[25] F. Cambeiro, E. Martínez-Núñez, J. A. Varela, C. Saá, *ACS Catalysis* **2015**, *5*, 6255-6262.

[26] a) M. S. Sanford, M. R. Valdez, R. H. Grubbs, *Organometallics* **2001**, *20*, 5455-5463; b) T. Braun, G. Münch, B. Windmüller, O. Gevert, M. Laubender, H. Werner, *Chem. Eur. J.* **2003**, *9*, 2516-2530.

[27] E. Peris, J. C. Lee, J. R. Rambo, O. Eisenstein, R. H. Crabtree, *J. Am. Chem. Soc.* **1995**, *117*, 3485-3491.

[28] For a recently described ruthenium η^3-furylcarbene, see: S. Peil, A. Fürstner, *Angew. Chem.* **2019**, *131*, 18647-18652; *Angew. Chem. Int. Ed.* **2019**, *58*, 18476-18481.

[29] a) S.-X. Luo, J. S. Cannon, B. L. H. Taylor, K. M. Engle, K. N. Houk, R. H. Grubbs, *J. Am. Chem. Soc.* **2016**, *138*, 14039-14046; b) J. R. Griffiths, J. B. Keister, S. T. Diver, *J. Am. Chem. Soc.* **2016**, *138*, 5380-5391.

[30] a) For previous proposals dealing with nucleophilic attacks of carbonyls to metal carbenes, see: J. A. Landgrebe, H. Iranmanesh; *J. Org. Chem.* **1978**, *43*, 1244-1245; b) A. C. Lottes, J. A. Landgrebe, K. Larsen, *Tetrahedron Lett.* **1989**, *30*, 4089-4092; c) M. Prein, A. Padwa, *Tetrahedron Lett.* **1996**, *37*, 6981-6984; d) M. Prein, P. J. Manley, A. Padwa, *Tetrahedron* **1997**, *53*, 7777-7794; e) M. Hamaguchi, H. Matsubara, T. Nagai, *Tetrahedron Lett.* **2000**, *41*, 1457-1460; f) J. Busch-Petersen, E. J. Corey, *Org. Lett.* **2000**, *2*, 1641-1643; g) M. P. Doyle, W. Hu, D. J. Timmons, *Org. Lett.* **2001**, *3*, 933-935; h) H. M. L. Davies, J. DeMeese, *Tetrahedron Lett.* **2001**, *42*, 6803-6805; i) A. E. Russell, J. Brekan, L. Gronenberg, M. P. Doyle, *J. Org. Chem.* **2004**, *69*, 5269-5274.

[31] Importantly, the hydrogen atom that undergoes the 1,5-hydrogen migration must be in *syn* disposition respect to the Cp*RuCl fragment as the activation energy for an *anti* migration was established in 64.3 kcal/mol (see Figure S12 in the Supporting Information for details).

[32] An alternative mechanism for the formation of vinyl epoxypyrrolidines from ylide **B** was also considered. However, no transition states could be located for the formation of the epoxide from this intermediate.

[33] a) A. B. Bortz, M. H. Kalos, J. L. Lebowitz, *J. Comput. Phys.* **1975**, *17*, 10-18; b) D. T. Gillespie, *J. Comput. Phys.* **1976**, *22*, 403-434.

[34] Deposition Number CCDC1973402 contains the supplementary crystallographic data for the compound **3b**. These data are provided free of charge by the joint Cambridge Crystallographic Data Centre and Fachinformationszentrum Karlsruhe Access Structures service www.ccdc.cam.ac.uk/structures

RESEARCH ARTICLE

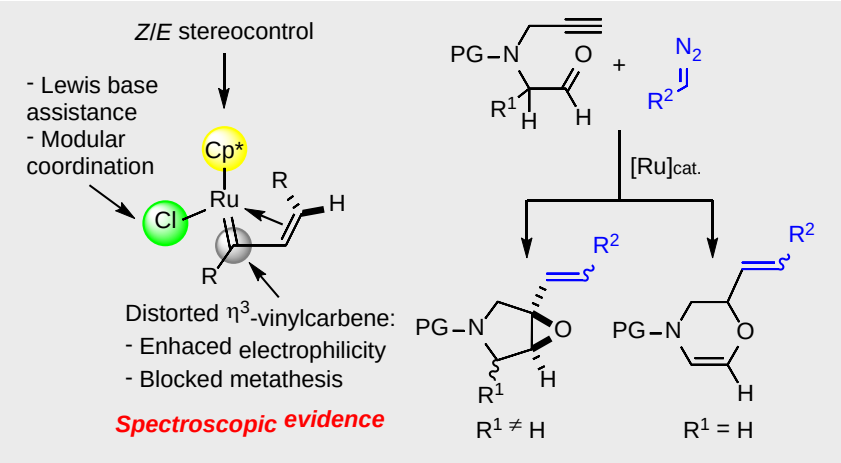

Damián Padín, Jesús A. Varela and Carlos Saá**

Page No. – Page No.

Cp*RuCl-Vinyl Carbenes: Two Faces and the Bifunctional Role in Catalytic Processes

A combination of spectroscopic and computational data shows that a distorted ruthenium η^3-vinylcarbene derived from a carbene/alkyne metathesis together with the Lewis basic chloride ligand generate two markedly different stereoelectronic faces that are responsible for their unconventional reactivity.